UC San Diego

Title

Body mass trajectories and cortical thickness in middle-aged men: a 42-year longitudinal study starting in young adulthood.

Permalink

https://escholarship.org/uc/item/08d220rj

Authors

Franz, Carol
Xian, Hong
Lew, Daphne
et al.

Publication Date

DOI

Peer reviewed

Body mass trajectories and cortical thickness in middle-aged men: A 42 year longitudinal study starting in young adulthood

Carol E. Franz[a], **Hong Xian**[b], **Daphne Lew**[b], **Sean N. Hatton**[a], **Olivia Puckett**[a], **Nathan Whitsel**[a], **Asad Beck**[c], **Anders M. Dale**[d], **Bin Fang**[a], **Christine Fennema-Notestine**[a,d], **Richard L. Hauger**[a,e], **Kristen C. Jacobson**[f], **Michael J. Lyons**[g], **Chandra A. Reynolds**[h], and **William S. Kremen**[a,e]

[a]Department of Psychiatry & Center for Behavior Genetics of Aging, University of California San Diego, La Jolla CA, USA

[b]Department of Epidemiology & Biostatistics, St. Louis University, St. Louis, MO, USA

[c]Department of Psychology, San Diego State University, San Diego, CA, USA

[d]Department of Radiology, University of California San Diego, La Jolla CA, USA

[e]Center of Excellence for Stress and Mental Health, VA San Diego Healthcare System, USA

[f]Department of Psychiatry & Behavioral Neuroscience, University of Chicago, Chicago, IL, USA

[g]Department of Psychological and Brain Sciences, Boston University, Boston, MA, USA

[h]Department of Psychology, University of California Riverside, Riverside, CA, USA

Abstract

Evidence strongly suggests that being overweight or obese at midlife confers significantly higher risk for Alzheimer's disease (AD) and greater brain atrophy later in life. Few studies, however, examine associations between longitudinal changes in adiposity during early adulthood and later brain morphometry. Measures of body mass index (BMI) were collected in 373 men from the Vietnam Era Twin Study of Aging at average age 20, 40, 56, and 62 years, yielding two BMI trajectories. We then examined associations between BMI phenotypes (trajectories, continuous BMI, obese/non-obese), cortical thickness, and white matter measures from structural magnetic resonance imaging at mean age 62 (Time 4, range 56-66). Those on the obesity trajectory (N=171) had thinner cortex compared with the normal/lean trajectory (N=202) in multiple frontal and temporal lobe bilateral regions of interest: superior, inferior, middle temporal gyri, temporal pole, fusiform gyrus, banks of the superior temporal sulcus, frontal pole, pars triangularis, caudal and rostral middle frontal gyri (all p<0.05 FDR corrected). Frontal lobe thinness tended to occur mainly in the right hemisphere. Results were similar for obese versus non-obese adults at age 62.

Other authors report no financial interests.

There were no significant differences for white matter volume or abnormalities. Taken in the context of other research, these associations between brain structure and excess BMI at midlife suggest potential for increased risk for cognitive decline in later life.

Keywords

obesity; body mass index (BMI); trajectory; longitudinal; cortical thickness; white matter abnormalities

1. Introduction

Obesity has long been established as a leading cause of morbidity and mortality among adults in the United States, with significantly worse cardiometabolic outcomes emerging as early as midlife (Grundy, 2004; Reilly and Kelly, 2011; Reis et al., 2015; Twig et al., 2016; Xian et al., 2017). Evidence strongly suggests that being overweight or obese at midlife also confers significantly higher risk for Alzheimer's disease (AD) and greater brain atrophy later in life (Albanese et al., 2017; Santos et al., 2017; Shaw et al., 2017; Shaw et al., 2018; Singh-Manoux et al., 2018). Chuang et al. (2016), for example, reported that each unit increase in body mass index (BMI) at midlife was associated with a 1-2% average brain tissue reduction in the frontal, temporal, and occipital lobes in late life, as well as with earlier onset of AD, greater Braak neurofibrillary tangle scores, and greater amyloid burden.

A major review of 44 studies concluded that greater adiposity (most frequently measured as BMI) is associated with smaller total gray matter (GM) volume; no consistent evidence was found, however, for adiposity effects on white matter volume or abnormalities (Willette and Kapogiannis, 2015). Findings varied by age (<40 versus 40+), gender, and measurement approach. The strongest results were for measures of categorical obesity rather than continuous BMI and for prefrontal, frontal, temporal and posterior cingulate regions. Many studies did not adjust for cardiovascular/cardiometabolic factors (Coutinho et al., 2017; Krishnadas et al., 2013; Walhovd et al., 2014). The majority of studies reviewed were cross-sectional, relatively small, focused on older adults, and examined global measures and cortical volumes. Thus, increased focus on specific brain regions and on younger adults is warranted.

Literature has also emerged showing that it is also important to examine thickness or surface area separately than simply focusing on cortical volume (Panizzon et al., 2009; Vuoksimaa et al., 2015). For instance, having a thinner cortex as adulthood progresses is thought to be related to degenerative processes due to key features such as organization of cortical layers, cell bodies in neurons, and synaptic connections, as well as cortical vulnerability to environmental influences (Fjell et al., 2014). Shaw et al. (2017) reported that increasing BMI over 8 years in 404 adults ages 44-49 predicted thinning in the posterior and caudal anterior cingulate, lingual gyrus, and pericalcarine regions of the cortex. In a two group study comparing the above 44-49 year old (midlife) adults with a group of 60-66 year-old (late life) adults, baseline BMI was associated with cortical thickness in late-life but not in midlife—most notably in the bilateral entorhinal cortex and bilateral cingulate (Shaw et al., 2018). Increasing BMI across 8 years was associated with cortical thinning in six lateral

regions of interest (ROIs) in the late-life group and one ROI in the midlife group. Medic et al (2016) found that among adults ages 18-50, two cortical regions (ventromedial prefrontal cortex and lateral occipital cortex) were significantly thinner in obese participants. Together these findings suggest that BMI-related brain differences typically found in older adults may already be present by midlife.

In the present study we examined relationships between BMI assessed four times across four decades starting at mean age 20 and cortical thickness, white matter volume, and white matter abnormalities in late midlife (approximately age 62). We predicted that adults on an obesity trajectory (where BMI rapidly increases toward obese levels) would be more likely than adults on a normal/lean BMI trajectory (where BMI stays relatively flat and close to normal levels) to have thinner cortices in frontal and temporal regions in late midlife. Analyses examined both bilateral and hemisphere-specific associations. In order to further elucidate these associations, we also conducted analyses with other BMI phenotypes: BMI measured continuously, and obese versus non-obese groups (BMI ≥ 30; BMI < 30). Next, we qualitatively visualized regions affected by BMI trajectories using exploratory vertex-wise cortical thickness analysis. Finally, we rigorously examined associations of BMI with white matter volume and white matter abnormalities. Along with the use of longitudinal BMI data, the inclusion of many factors like hypertension, fasting glucose, triglyceride, cholesterol, and C-reactive protein is a strength of the study.

2. Material and methods

2.1. Participants

Participants were from the Vietnam Era Twin Study of Aging (Kremen et al., 2013b), a longitudinal study of risk and protective factors for cognitive and brain aging in a communitydwelling sample of men from across the United States (U.S.). VETSA participants were recruited as a simple random sample from the all-male Vietnam Era Twin Registry (VETR) (Goldberg et al., 2002), a research registry of twins who all served in the U.S. military sometime between 1965 and 1975. VETSA 1 (2002-2008) eligibility included being 51 to 59 years old when recruited and both members of a twin pair agreed to participate (Kremen et al., 2006). The VETSA 2 (2009-2013) follow-up occurred approximately 6 years later (Kremen et al., 2013). VETSA participants comprise a representative epidemiological sample of community-based men with regard to marital, work, income, and health characteristics of American men in their age range based on U.S. Census and Center for Disease Control data (CDC) (Schoenborn and Heyman, 2009). As a sample of veterans, at baseline, VETSA participants constitute a group with no major chronic childhood health problems. The military recruitment standards mandate weight-for-height and maximum body fat limits (with occasional waivers for under- or overweight recruits), thus the majority of the participants were not obese at baseline (98%)(Cawley and Maclean, 2012). Nearly 80% of VETSA participants report no combat experience. More details about the VETSA MRI sample and data collection are published elsewhere (Fennema-Notestine et al., 2016; Kremen et al., 2013a).

2.2. Procedures.

This study utilizes BMI data collected from the same participants at four timepoints: baseline (Time 1; mean age 19.9 years, SD=1.4; range 18-24); a 1990 National Heart, Lung, and Blood Institute survey (Time 2; mean age 40.3, SD=2.7; range 35-44) (Goldberg et al., 2002) and in-person evaluations at either the University of California San Diego (UCSD) or Boston University (BU) at VETSA 1 (Time 3; mean age 56.3, SD=2.6; range 51-60) and VETSA 2 (Time 4; mean age 61.9, SD=2.6; range 56-66). On the day following the Time 4 in-person assessment, the subsample of MRI eligible participants (N=426) underwent structural magnetic resonance imaging (MRI) at either UCSD or Massachusetts General Hospital (MGH).

Institutional review board approval was obtained at all sites and participants provided written informed consent.

2.3. Measures.

2.3.1 BMI.—Height and weight were objectively measured at Times 1, 3 and 4 as part of physical examinations. Time 1 occurred at the military induction physical. Time 2 height and weight were self-reported as part of a mailed survey. Self-reported height and weight are considered valid measures, but can be biased depending on age, gender, and ethnicity (Connor-Gorber et al., 2007; Richmond et al., 2015). At Times 3 and 4, participants were weighed inperson on a digital scale after removing shoes, heavy outer clothing, and pocket items. Height was assessed, in stocking feet, with a stadiometer. After transforming height and weight to metric units, BMI was calculated as kg/m^2. As reported earlier, height was highly correlated across Times 2,3,4 when full adult height had been reached (Xian et al., 2017).

BMI trajectories were derived previously (Xian et al., 2017) using continuous measures of BMI and latent class growth modeling (LCGM) in Mplus version 7.4 (Muthen and Muthen, 2015). In LCGM, each participant receives a membership probability for each mutually exclusive trajectory based on the BMI change pattern over time and is assigned to the trajectory with the highest probability. Although three BMI trajectories across the 4 timepoints were identified in the full sample (Xian et al., 2017), one group contained only 13 participants in the MRI subsample. For these analyses we combined the two trajectories with rapidly increasing BMI; because both ended in obesity, we call this combined trajectory the obesity trajectory (N=171). The group that maintained BMI with a relatively flat slope remaining close to normal BMI range across the four decades we called the normal BMI trajectory (N=202; see Table 1 for descriptive information). BMI was the only indicator of adiposity available at all four timepoints. Separate measures of obese/not obese (BMI 30; BMI < 30 respectively) were created at each time point.

2.3.2. MRI acquisition and processing.

2.3.2.1 Cortical thickness and white matter volume.: At Time 4, T1-weighted images were acquired on a GE 3T Discovery 750 scanner (GE Healthcare, Waukesha, WI, USA) with an 8-channel phased array head coil at UCSD, and a Siemens Tim Trio, (Siemens USA, Washington, D.C.) with a 32-channel head coil at MGH . At UCSD, the 3D fast spoiled

gradient echo (FSPGR) T1-weighted image protocol was: TE=3.164 msec, TR=8.084 msec, TI=600 msec, flip angle=8°, pixel bandwidth=244.141, FOV=24 cm, frequency=256, phase=192, slices=172, slice thickness=1.2 mm. At MGH, the 3D magnetization-prepared rapid gradient echo (MPRAGE) T1-weighted image protocol was: TE=4.33 msec, TR=2170 msec, TI=1100 msec, flip angle=7°, pixel bandwidth=140, slices=160, slice thickness=1.2 mm.

Raw image files were processed using an automated stream developed by the UCSD Center for Multimodal Imaging and Genetics under the direction of Dr. Dale. Images were corrected for gradient distortions (Jovicich et al., 2006) and B1 field inhomogeneity (Sled et al., 1998). Any images with severe scanner artifacts or excessive head motion were excluded (see section 2.3.2.3). T1-weighted images were then processed via the FreeSurfer v5.1 pipeline (Fischl, 2012) for white matter volume and for cortical parcellation data derived from the Desikan-Killiany Atlas (Desikan et al., 2006). All processed images were visually reviewed for quality, and the cortical surface related images were edited for technical accuracy in alignment with standard, objective rules to improve the brain mask (removing non-brain voxels) and white matter volume (filling hyperintense white matter lesions).

2.3.2.2.   White matter abnormalities.: Measured white matter abnormalities may include white matter hyperintensities of presumed vascular origin, lacunes, and small subcortical infarcts (all hyperintense on T2-weighted or FLAIR and iso- or hypo-intense regions on T1) (Fennema-Notestine et al., 2016). To examine white matter lesion load, T2- and PD-weighted images also were acquired in the same session. At UCSD the T2-weighted coronal 2D FRFSE-XL protocol was: TE=94 msec, TR=4.6 sec, flip angle=90°, pixel bandwidth=122, FOV=24cm, frequency=256, phase=256, slices=96, slice thickness=2mm, ETL=16, NEX=2. The PD-weighted coronal 2D FSE-XL protocol was: TE=13 msec, TR=3 sec, flip angle=90°, pixel bandwidth=122, FOV=24cm, frequency=256, phase=256, slices=96, slice thickness=2mm, ETL=4, NEX=1. At MGH the T2-weighted coronal 2D TSE protocol was: TE=93 msec, TR=4.7 sec, flip angle=116°, pixel bandwidth=219, FOV=24cm, frequency=123, phase=92, slices=96, slice thickness=2mm, ETL=24, NEX=2. The PD-weighted coronal 2D TSE protocol was: TE=19 msec, TR=3 sec, flip angle=116°, pixel bandwidth=219, FOV=24cm, frequency= 23, phase=192, slices=96, slice thickness=2mm, ETL=12, NEX=2.

White matter abnormality volume was determined using a multi-channel (T1-, T2- and PD-weighted) segmentation approach (Fennema-Notestine et al., 2016). The T1 image was rigidly aligned to standard space, then the T2 and PD images were registered to the T1 and nonparametric non-uniform intensity normalization (N3) bias-corrected (Sled et al., 1998). A 3-class tissue segmentation calculated the robust means and covariances for white matter, gray matter, and CSF. Abnormal voxel clusters were identified as voxels originally segmented as gray matter that were situated within anatomically defined white matter regions. All results were visually reviewed, and misclassifications were manually corrected. Volumes were measured in each participant's native (undeformed) space. To avoid misclassification due to partial voluming errors, any voxels that touched (i.e., shared a common face, edge, or vertex with) a ventricular fluid voxel were excluded from all analyses.

2.3.2.3. MRI scan exclusion criteria.: Initially there was a total of 416 cases available that acquired all three scans (T1, T2, PD). From this, 4.3% (n=18) were excluded for motion artifact degrading quality in one or more of the three scans and 25 additional cases (4.7% at BU and 5.4% at UCSD) were excluded due to poor image processing information (including 3 with medical conditions that made for poor segmentation) that could not be resolved by standard manual intervention. The proportion did not differ by site for either reason. A final total of 373 participants with complete MRI data remained in the analytic sample.

2.3.3. Covariates.—Covariates included in analyses were age, lifetime education, ethnicity, smoking status and being at-risk for hypertension, dyslipidemia, diabetes, inflammation, and/or ischemic heart disease at Time 4. Blood pressure was based on the average of four systolic (SBP) diastolic (DBP) blood pressure readings taken during the assessment day. Individuals with either SBP > 140 or DBP > 90 mm Hg (Aronow et al., 2011), or who took anti-hypertensive medication, were classified as at-risk for hypertension (75.1%). Fasting plasma glucose was assayed with spectrophotometry as part of a comprehensive metabolic panel; glucose levels > 5.54 mmol/L (comparable to 100 mg/dl) were considered at-risk. Being at-risk for diabetes was defined as having at-risk levels of glucose, and/or taking a prescription medication for diabetes (51.7%) as per the International Diabetes Federation global consensus: (http://www.idf.org/webdata/docs/ IDF_Meta_def_final.pdf). Triglycerides and HDL-cholesterol were assayed as part of a lipid panel via spectrophotometry. At-risk HDL-cholesterol was defined as levels < 1.03 mmol/L (28.9%); at-risk triglycerides was classified as > 1.68 mmol/L (31.5%). At-risk overall cholesterol was defined as being at-risk for either HDL or triglycerides or taking cholesterol-lowering medication (72% at-risk) (Grundy, 2004). High-sensitivity C-reactive protein (CRP), a protein measured in blood that indicates inflammation, was assayed using nephelometry (Mora et al., 2009) and at-risk inflammation was defined as CRP > 28.5 nmol/L (27.5%). Presence/absence of ischemic heart disease at Time 4 (18%) was coded using a validated population-based index (Xian et al., 2010) indicating presence of angina based on a positive Rose Angina score and/or a prescription for nitroglycerin (Lampe et al., 1999), self-reported heart attack/myocardial infarction, and/or heart surgery. Ethnicity was coded as white non-Hispanic versus other. Tobacco smoking was coded as never, former or current. Lifetime education reflected the number of years of formal schooling completed (e.g., secondary school diploma=12; 4-year college degree=16; PhD/MD=20).

2.4. Data analyses.

2.4.1. Linear mixed model analyses.—Left and right hemisphere ROI measures were averaged to obtain bilateral ROI measures. Because different scanners were used at the two sites, all MRI measures adjusted for scanner. Cortical thickness measures also adjusted for weighted mean cortical thickness, calculated as the sum of all cortical volume ROIs divided by the total surface area. These ROIs were then used in the linear mixed model statistical analyses. White matter measures were adjusted for intracranial volume to account for individual differences in head size. Analyses included the random effect of family to account for the twin clustering of the data and covariates described in section 2.3.3..

Linear mixed models were used to examine associations between neuroimaging measures and BMI phenotypes. Statistical analyses used Proc Mixed in SAS version 9.4 (SAS Institute, Cary, North Carolina). We followed up the BMI trajectory comparisons of ROIs with vertex-wise analyses and hemisphere-based analyses, including the same covariates. Finally, we examined associations between obese/non-obese groups and continuous BMI with the cortical thickness continuous measures at Time 4. All *p*-values are 2-tailed. Results reflect false discovery rate (FDR) corrections at p<.05 (two-tailed) for multiple comparisons (Benjamini and Hochberg, 1995; Li and Ji, 2005).

2.4.2. Vertex-wise analyses.—We conducted an exploratory vertex-wise analysis to qualitatively examine regions of the cortex that could be affected by BMI, by hemisphere. This offered a visual perspective of the regions affected, but is limited by the constraints of the generalized linear model which does not permit the inclusion of missing data or random effects (i.e. twin relatedness) which linear mixed models can incorporate.

Cortical vertex-wise analysis in conducted in Matlab r2014a using the Matlab FreeSurfer and Statistical toolboxes. Cortical thickness maps for each hemisphere were concatenated and a general linear mixed model was run contrasting the BMI trajectories (different intercept, different slope) while controlling for education, ethnicity, age, and being at-risk for dyslipidemia, hypertension, diabetes or ischemic heart disease, and scanner. To improve sensitivity and signal to noise ratio, we applied a 30 mm full wide half maximum (FWHM) smoothing kernel recommended for cortical thickness (Lerch and Evans, 2005). It should be noted that this smoothing does inherently reduce specificity and anatomical precision (Bernal-Rusiel et al., 2010). Significance was set at *p*<.05 (FDR-corrected) for clusters larger than 100 voxels and statistical maps were rendered over the FreeSurfer average brain.

3.   Results

3.1.   Descriptive results.

Comparisons between normal BMI and obesity trajectories revealed no differences in cognitive ability at Time 1 (average age 20), education, or age (see Table 1). The normal BMI trajectory (N=202) was significantly more likely to be white non-Hispanic (91%) compared with the obesity trajectory (83%). Mean BMI in the obesity trajectory (N=171) was significantly higher at all four timepoints. As shown in Table 1, compared with the normal BMI trajectory, members of the obesity trajectory were more likely to have at-risk levels of CRP, diabetes, SBP and DBP at Time 4 (average age 62). Risk for metabolic syndrome—that is, the co-occurrence of 3 or more cardiometabolic risk indicators (i.e., at-risk for obesity, dyslipidemia, hypertension, diabetes)—occurred more frequently in the obesity trajectory (59.4%) compared with the normal BMI trajectory (17.4%). Rates of ischemic heart disease or smoking were not significant.

3.2.   BMI trajectories and bilateral ROI cortical thickness.

The obesity trajectory compared with the normal BMI trajectory had significantly thinner cortex in multiple bilateral frontal ROIs (i.e., frontal pole, pars triangularis, caudal and rostral middle frontal gyri ROIs) and temporal lobe (i.e., banks of the superior temporal

sulcus; inferior, middle, and superior temporal gyri; fusiform gyrus; temporal pole) (Table 2, Figure 1). No regions in the cingulate, occipital lobe, or parietal lobe were different after FDR correction.

3.3. Obese/non-obese group comparisons, continuous BMI, and bilateral ROI cortical thickness.

We examined the extent to which categorical BMI (obese/not obese) or continuous BMI at each timepoint, adjusted for all covariates, were associated with cortical thickness at Time 4. Obesity at Time 1 or 3 (average age 56) did not predict any midlife brain outcome. At Time 2 (average age 40), 1 comparison survived FDR correction: the obese group had a significantly thicker lateral occipital gyrus than the non-obese group (Supplemental Table 1).

Within Time 4, comparisons of obese versus non-obese groups closely paralleled those for the trajectory analyses, showing group differences largely in the frontal and temporal lobes (Table 3). The obese group had thinner pars triangularis, caudal and rostral middle frontal gyri, precentral gyrus, banks of the superior temporal sulcus, middle and superior temporal gyri, and fusiform gyrus compared with the non-obese group (supplemental Figure 1). The supramarginal gyrus of the parietal lobe was significantly thinner in the obese group. No results were significant at any time for the continuous BMI measure (data not shown).

Finally, post-hoc we ran mixed effect models by hemisphere that excluded cardiometabolic risk measures (i.e., at-risk hypertension, dyslipidemia, diabetes, inflammation, ischemic heart disease) as covariates (see supplemental Tables 2 and 3). Point estimates were largely similar suggesting that most of the association is explained by BMI.

3.4. Lateralized cortical thickness.

We first conducted an exploratory vertex-wise analysis to qualitatively examine regions of the cortex that could be affected by BMI, using generalized linear models. As can be seen in Figure 2, the vertex-wise analyses show the obesity trajectory with significantly thinner cortex (p<0.05, FDR corrected) in clusters representing the right medial superior frontal cortex, right pars opercularis, right pars triangularis, right caudal middle frontal gyri, right and left rostral middle frontal gyri, left isthmus, left rostral anterior cingulate as well as in both right and left temporal lobes and fusiform gyri (Figure 2; regions in blue have t-test thresholds > 2).

3.4.1. BMI trajectories and hemisphere-specific ROI cortical thickness.—We then examined associations between BMI phenotypes and cortical ROIs, separately by hemisphere, using mixed models with all covariates and the random effect of twin. In the right hemisphere, the obesity trajectory compared with the normal trajectory group had thinner cortex in the precentral gyrus, pars opercularis, pars triangularis, caudal and rostral midfrontal gyri, middle and superior temporal gyri, and temporal pole (Table 2). In the left hemisphere, the obese trajectory had significantly thinner banks of the superior temporal sulcus, inferior and middle temporal cortex, and fusiform gyrus compared with the normal trajectory. No regions in the right or left cingulate, occipital, or parietal lobes or in the left frontal lobe were significant after FDR-correction.

3.4.2. Obese/non-obese groups at Time 4 and hemisphere-specific ROI cortical thickness.—With regard to obese/non-obese group comparisons at Time 4 (Table 3), the obese group had thinner right precentral gyrus, right pars triangularis, right caudal and rostral middle frontal gyri, right postcentral gyrus, right supramarginal gyrus, right middle and superior temporal gyri, and right temporal pole as well as left banks of superior temporal sulcus, left inferior and middle temporal cortex, and left fusiform gyrus compared to the non-obese group. Of interest in the obese/non-obese comparisons is the emergence of significant differences in two right parietal ROIs (Postcentral gyrus, supramarginal gyrus) that had not remained significant after FDR correction in the trajectory analyses. There were no significant associations between BMI measured continuously at age 62 and lateralized cortical thickness ROIs (data not shown).

3.5. White matter volume and abnormalities.

There were no significant associations between trajectory group and total white matter volume (β=0.0001, p=.98) or abnormal white matter volume (β=−.0097, p=.91). Associations between Time 4 obesity and total white matter volume (β=−.0003, p=.97) or abnormal white matter volume (β=−.0200, p=.85) were not significant (or at other timepoints, data not shown).

4. Discussion

Among men who were healthy, trajectories with steeper increases in continuously measured BMI across 4 decades were associated with having thinner cortices in late midlife, predominantly in temporal and frontal regions, despite most of these men having BMI in the normal range at the age 20 baseline. Cross-sectional results for obesity—but not continuously measured BMI—at age 62 closely paralleled those for BMI trajectory. Results for the frontal lobe appeared primarily in the right hemisphere; cortical thinness in the temporal lobe occurred in both hemispheres. Having a thinner cortex in temporal regions has most strongly predicted dementia-related outcomes in some studies. McEvoy et al. reported that temporal lobe thinning predicted more rapid onset of mild cognitive impairment and/or AD-like dementias (McEvoy et al., 2009). In a study of eight AD-related cortical regions in middle-aged adults, Pettigrew et al. (2016) found that overall thinness in those regions predicted development of clinical AD symptoms and tau pathology across seven years; four of the seven regions overlapped our temporal lobe regions (Pettigrew et al., 2016). Comparable to a number of other studies, BMI as a continuous measure was not associated with cortical thickness. This suggests that being obese by late midlife is likely the more salient BMI phenotype related to the brain outcomes.

Longitudinal studies of BMI and cortical thickness in adults from young adulthood to late midlife are rare. In one other longitudinal study of adults in their 40s (Shaw et al., 2017), increasing BMI across 8 years was associated with thinning in the posterior cingulate (bilaterally), as well as thinning in the right lingual gyrus, anterior cingulate, and pericalcarine sulcus (p<.05, one-sided) in vertex-wise analyses. Shaw et al. (2018) further reported that baseline BMI in 60-66 year-olds, but not 40 year-olds, was associated with cortical thickness 8 years later—most notably in the bilateral entorhinal cortex and bilateral

cingulate. Increasing BMI across 8 years was associated with cortical thinning in multiple lateralized ROIs mainly in the late-life group. Our analyses only found thinner cortex in portions of the cingulate in the vertex-wise analyses and in the right hemisphere of obese participants. Overall our strongest results were in the temporal and frontal regions. It may be that the differences are due to participant characteristics such as gender (VETSA is all male, the Shaw sample was approximately 54% female), age, or study duration (42 years versus eight years). Nevertheless, these results suggest that the effects of excessive adiposity and associated processes on the brain likely start appearing by midlife. It is unknown if these effects are reversible; previous research found that caloric restriction improved memory performance in older adults; it is possible reasonable reduction in BMI within could have an effect on cortical thickness (Witte et al., 2009).

While the obesity paradox—the controversial finding by some researchers that while high midlife BMI increases risk for cognitive decline and dementia, higher late-life BMI may be protective—is often studied with regard to cognition, it is less often examined in brain phenotypes. This study finds support for an association between the role of excess BMI by late midlife and brain vulnerability. Shaw et al. (2018) compared younger and older groups as a way of elucidating the paradox. Consistent with the paradox, increasing BMI was associated with greater cortical thinning over time (primarily in the older group); however, decreasing BMI across eight years in the older group, but not the younger group, was also associated with greater cortical thinning in multiple ROIs. Among older adults with AD, however, Malpetti et al.(2018) reported that having a higher BMI was associated with greater brain vulnerability for women but not men, finding no evidence that higher BMI was protective; brain vulnerability was defined as brain hypometabolism and lower metabolic connectivity in key resting-state networks. In our analyses, we found no evidence for high BMI as being protective. Given that the age range of our sample falls between those of the Shaw et al. groups, this is perhaps not unexpected and may be due to the relatively young age (average age 62) or high levels of BMI. In future studies, however, a longitudinal design combined with early measures of BMI and brain will help to elucidate the obesity paradox and how risks associated with BMI may change across the life course as well as illuminate the roles of factors such as health, age, and selective attrition, among others, in this phenomenon.

Finally, although some studies find associations between BMI and white matter abnormalities, there were no significant associations in our analyses. Causes of white matter abnormalities include vasculopathy, demyelination, and gliosis, but the most common cause associated with aging and cerebrovascular disease is ischemic pathogenesis, or small cerebral vessel disease (Fennema-Notestine et al., 2016; Santos, P.P. et al., 2017). It may be the VETSA participants are too young (average age 62) to detect these associations. Additionally, the sample had low rates of ischemic heart disease.

A number of mechanisms may link excessive midlife BMI with neurodegenerative damage; these likely are interlinked mechanisms that include vascular and metabolic pathways, inflammatory processes, and possibly genetic influences. BMI is strongly associated with poor outcomes on cardiometabolic and cardiovascular measures (Grundy, 2004; Reilly and Kelly, 2011; Reis et al., 2015; Twig et al., 2016; Xian et al., 2017). Our analyses controlled

for multiple risks for cardiometabolic disease and still found significant associations between BMI trajectory and/or obesity with cortical thickness at midlife. Higher levels of BMI may also decrease cerebral blood flow and cardiac output distribution to the brain with age (Xing et al., 2017). Studies of the lipidome suggest that complex interactive processes are involved with body mass, lipid dynamics, cell metabolism, and brain morphology; lipids have essential roles in cellular signaling and membrane protein assembly and AD progression is strongly associated with abnormal lipid metabolism (Li et al., 2017; Nam et al., 2017). Epigenetic mechanisms such as those involved in DNA methylation may also be involved; a study of the Dutch Hunger Winter, for example, found that epigenetic factors mediated associations between exposure to adversity during early development and BMI in adulthood (Tobi et al., 2018). Such risk factors are also likely to play a role in brain development. Explorations of the substantial genetic overlap between cardiometabolic indicators, inflammation, and BMI may also yield further insights into the biology of obesity, neurodegenerative damage, and comorbidity with other disease processes (Locke et al., 2015; Marioni et al., 2016; Panizzon et al., 2015; Santos, C.Y. et al., 2017). For instance, in a genome-wide association study meta-analysis, the most strongly enriched gene sets for BMI and obesity involved critical brain pathways regulating appetite, insulin synthesis and processing, and energy metabolism in the hypothalamus and pituitary, synaptic plasticity and cellular mechanisms (Locke et al., 2015). Genetic analyses were beyond the scope of this study.

Our study has several limitations. Longitudinal MRI data were not available so we were unable to evaluate whether the brain structures were different at earlier time periods. Scanner selection criteria typically exclude extremely heavy men (i.e., girth greater than the MRI bore and/or, in these scanners, weight greater than 300 pounds), which restricts examination of brain phenotypes in more extreme cases. Studies focused on older adults, however, likely already have high levels of selective attrition associated with obesity related to both health and scanner limitations. Waist circumference is sometimes considered a better indicator of adiposity than BMI (Connor-Gorber et al., 2007), but BMI was our only measure with multiple timepoints, which allowed for trajectory and longitudinal analyses. Moreover, BMI and waist circumference in the present sample were correlated r=0.90. BMI data at Time 2 was self-reported; mis-estimation of self-reported BMI has been shown in different groups (Richmond et al., 2015). The sample is primarily male non-Hispanic white veterans, so generalizability to women and other groups is unclear. Recent longitudinal studies find some sex differences in associations with BMI (von Bonsdorff et al., 2015). A strength of the study includes the homogeneity of age in an allmale sample, thereby increasing our power.

4.1   Conclusions.

To our knowledge, this study is unique in its analyses of four decades of longitudinal BMI data starting in young adulthood and the relationship of BMI phenotypes with cortical thickness and white matter in late midlife. This large age-homogeneous sample allowed for in-depth examination of BMI change and heterogeneity across an important transitional age period when cardiometabolic dysregulation and inflammation become more prevalent (Locke et al., 2015). We provided evidence that either steeply increasing BMI from young adulthood to late midlife or obesity in late midlife is significantly associated with thinner

cortex in late midlife, predominantly in the frontal and temporal lobes. Results for the BMI trajectory and Time 4 obesity analyses were comparable, so there appears to be no statistical advantage to examining trajectories over current obesity. In contrast to the BMI trajectories, however, continuously measured BMI at Time 4 was not associated with cortical thickness. Knowing what trajectory a person is on earlier in adulthood may also be clinically useful (Croswell and Luger, 2012). Taken in the context of other research, these associations with excess BMI at midlife portend potentially increased risk for cognitive decline (Albanese et al., 2017; Chuang et al., 2016) and reduced life expectancy in later life (Olshansky et al., 2005).

Supplementary Material

Refer to Web version on PubMed Central for supplementary material.

5. References

Albanese E, Launer LJ, Egger M, Prince MJ, Giannakopoulos P, Wolters FJ, Egan K, 2017 Body mass index in midlife and dementia: Systematic review and meta-regression analysis of 589,649 men and women followed in longitudinal studies. Alzheimers Dement (Amst) 8, 165–178. [PubMed: 28761927]

Aronow WS, Fleg JL, Pepine CJ, Artinian NT, Bakris G, Brown AS, Ferdinand KC, Forciea MA, Frishman WH, Jaigobin C, Kostis JB, Mancia G, Oparil S,Ortiz E, Reisin E, Rich MW, Schocken DD, Weber MA, Wesley DJ, Harrington RA, 2011 ACCF/AHA 2011 expert consensus document on hypertension in the elderly: a report of the American College of Cardiology Foundation Task Force on Clinical Expert Consensus Documents. Circulation 123(21), 2434–2506. [PubMed: 21518977]

Benjamini Y, Hochberg Y, 1995 Controlling the False Discovery Rate: A Practical and Powerful Approach to Multiple Testing. J R Stat Soc Series B Stat Methodol 57, 289–300.

Bernal-Rusiel JL, Atienza M, Cantero JL, 2010 Determining the optimal level of smoothing in cortical thickness analysis: a hierarchical approach based on sequential statistical thresholding. Neuroimage 52(1), 158–171. [PubMed: 20362677]

Cawley J, Maclean JC, 2012 Unfit for Service: The Implications of Rising Obesity for U.S. Military Recruitment. Health Econ. 21, 1348–1366. [PubMed: 21971919]

Chuang YF, An Y, Bilgel M, Wong DF, Troncoso JC, O'Brien RJ, Breitner JC, Ferruci L, Resnick SM, Thambisetty M, 2016 Midlife adiposity predicts earlier onset of Alzheimer's dementia, neuropathology and presymptomatic cerebral amyloid accumulation. Mol Psychiatry 21(7), 910–915. [PubMed: 26324099]

Connor-Gorber S, Tremblay A, Moher D, Gorber B, 2007 A comparison of direct vs. self-report measures for assessing height, weight and body mass index: a systematic review. Obes Rev 8, 307–326. [PubMed: 17578381]

Coutinho AM, Coutu JP, Lindemer ER, Rosas HD, Rosen BR, Salat DH, 2017 Differential associations between systemic markers of disease and cortical thickness in healthy middle-aged and older adults. Neuroimage 146, 19–27. [PubMed: 27847345]

Croswell J, Luger S, 2012 Screening for and management of obesity in adults. Am. Fam. Physician 86(10), 947–948. [PubMed: 23157148]

Desikan RS, Segonne F, Fischl B, Quinn BT, Dickerson BC, Blacker D, Buckner RL, Dale AM, Maguire RP, Hyman BT, Albert MS, Killiany RJ, 2006 An automated labeling system for subdividing the human cerebral cortex on MRI scans into gyral based regions of interest. Neuroimage 31, 968–980. [PubMed: 16530430]

Fennema-Notestine C, McEvoy LK, Notestine R, Panizzon MS, Yau WW, Franz CE, Lyons MJ, Eyler LT, Neale MC, Xian H, McKenzie RE, Kremen WS, 2016 White matter disease in midlife is heritable, related to hypertension, and shares some genetic influence with systolic blood pressure. Neuroimage Clin 12, 737–745. [PubMed: 27790395]

Fischl B, 2012 FreeSurfer. Neuroimage 62(2), 774–781. [PubMed: 22248573]

Fjell AM, Westlye LT, Grydeland H, Amlien I, Espeseth T, Reinvang I, Raz N, Dale AM, Walhovd KB, Alzheimer Disease Neuroimaging I, 2014 Accelerating cortical thinning: unique to dementia or universal in aging? Cereb. Cortex 24(4), 919–934. [PubMed: 23236213]

Goldberg J, Curran B, Vitek ME, Henderson WG, Boyko EJ, 2002 The Vietnam Era Twin Registry. Twin Res. 5(5), 476–481. [PubMed: 12537880]

Grundy SM, 2004 Obesity, metabolic syndrome, and cardiovascular disease. J. Clin. Endocrinol. Metab. 89(6), 2595–2600. [PubMed: 15181029]

Jovicich J, Czanner S, Greve D, Haley E, van der Kouwe A, Gollub R, Kennedy D, Schmitt F, Brown G, Macfall J, Fischl B, Dale AM, 2006 Reliability in multi-site structural MRI studies: Effects of gradient non-linearity correction on phantom and human data. Neuroimage 30, 436–443. [PubMed: 16300968]

Kremen WS, Fennema-Notestine C, Eyler LT, Panizzon MS, Chen CH, Franz CE, Lyons MJ, Thompson WK, Dale AM, 2013a Genetics of brain structure: contributions from the Vietnam Era Twin Study of Aging. American Journal of Medical Genetics Part B Neuropsychiatric Genetics 162B(7), 751–761.

Kremen WS, Franz CE, Lyons MJ, 2013b VETSA: the Vietnam Era Twin Study of Aging. Twin Research and Human Genetics 16(1), 399–402. [PubMed: 23110957]

Kremen WS, Thompson-Brenner H, Leung YM, Grant MD, Franz CE, Eisen SA, Jacobson KC, Boake C, Lyons MJ, 2006 Genes, environment, and time: the Vietnam Era Twin Study of Aging (VETSA). Twin Res Hum Genet 9(6), 1009–1022. [PubMed: 17254445]

Krishnadas R, McLean J, Batty GD, Burns H, Deans KA, Ford I, McConnachie A, McGinty A, McLean JS, Millar K, Sattar N, Shiels PG, Velupillai YN, Packard CJ, Cavanagh J, 2013 Cardio-metabolic risk factors and cortical thickness in a neurologically healthy male population: Results from the psychological, social and biological determinants of ill health (pSoBid) study. Neuroimage Clin 2, 646–657. [PubMed: 24179815]

Lampe FC, Walker M, Lennon LT, Whincup PH, Ebrahim S, 1999 Validity of a self-reported history of doctor-diagnosed angina. J. Clin. Epidemiol. 52(1), 73–81. [PubMed: 9973076]

Lerch JP, Evans AC, 2005 Cortical thickness analysis examined through power analysis and a population simulation. Neuroimage 24(1), 163–173. [PubMed: 15588607]

Li J, Ji L, 2005 Adjusting multiple testing in multilocus analyses using the eigenvalues of a correlation matrix. Heredity (Edinb.) 95(3), 221–227. [PubMed: 16077740]

Li Q, Bozek K, Xu C, Guo Y, Sun J, Paabo S, Sherwood CC, Hof PR, Ely JJ, Li Y, Willmitzer L, Giavalisco P, Khaitovich P, 2017 Changes in Lipidome Composition during Brain Development in

Humans, Chimpanzees, and Macaque Monkeys. Mol. Biol. Evol. 34(5), 1155–1166. [PubMed: 28158622]

Locke AE, Kahali B, Berndt SI, Justice AE, Pers TH, Day FR, Powell C, Vedantam S, Buchkovich ML, Yang J, Croteau-Chonka DC, Esko T, Fall T, Ferreira T, Gustafsson S, Kutalik Z, Luan J, Magi R, Randall JC, Winkler TW, Wood AR, Workalemahu T, Faul JD, Smith JA, Hua Zhao J, Zhao W, Chen J, Fehrmann R, Hedman AK, Karjalainen J, Schmidt EM, Absher D, Amin N, Anderson D, Beekman M, Bolton JL, Bragg-Gresham JL, Buyske S, Demirkan A, Deng G, Ehret GB, Feenstra B, Feitosa MF, Fischer K, Goel A, Gong J, Jackson AU, Kanoni S, Kleber ME, Kristiansson K, Lim U, Lotay V, Mangino M, Mateo Leach I, Medina-Gomez C, Medland SE, Nalls MA, Palmer CD, Pasko D, Pechlivanis S, Peters MJ, Prokopenko I, Shungin D, Stancakova A, Strawbridge RJ, Ju Sung Y, Tanaka T, Teumer A, Trompet S, van der Laan SW, van Setten J, Van Vliet-Ostaptchouk JV, Wang Z, Yengo L, Zhang W, Isaacs A, Albrecht E, Arnlov J, Arscott GM, Attwood AP, Bandinelli S, Barrett A, Bas IN, Bellis C, Bennett AJ, Berne C, Blagieva R, Bluher M, Bohringer S, Bonnycastle LL, Bottcher Y, Boyd HA, Bruinenberg M, Caspersen IH, Ida Chen YD, Clarke R, Daw EW, de Craen AJ, Delgado G, Dimitriou M, Doney AS, Eklund N, Estrada K, Eury E, Folkersen L, Fraser RM, Garcia ME, Geller F, Giedraitis V, Gigante B, Go AS, Golay A, Goodall AH, Gordon SD, Gorski M, Grabe HJ, Grallert H , Grammer TB, Grassler J, Gronberg H, Groves CJ, Gusto G, Haessler J, Hall P, Haller T, Hallmans G, Hartman CA, Hassinen M, Hayward C, Heard-Costa NL, Helmer Q, Hengstenberg C, Holmen O, Hottenga JJ, James AL, Jeff JM, Johansson A, Jolley J, Juliusdottir T, Kinnunen L, Koenig W, Koskenvuo M, Kratzer W, Laitinen J, Lamina C, Leander K, Lee NR, Lichtner P, Lind L, Lindstrom J, Sin Lo K, Lobbens S, Lorbeer R, Lu Y, Mach F, Magnusson PK, Mahajan A, McArdle WL, McLachlan S, Menni C, Merger S, Mihailov E, Milani L, Moayyeri A, Monda KL, Morken MA, Mulas A, Muller G, Muller-Nurasyid M, Musk AW, Nagaraja R, Nothen MM, Nolte IM, Pilz S, Rayner NW, Renstrom F, Rettig R, Ried JS, Ripke S, Robertson NR, Rose LM, Sanna S, Scharnagl H, Scholtens S, Schumacher FR, Scott WR, Seufferlein T, Shi J, Vernon Smith A, Smolonska J, Stanton AV, Steinthorsdottir V, Stirrups K, Stringham HM, Sundstrom J, Swertz MA, Swift AJ, Syvanen AC, Tan ST, Tayo BO, Thorand B, Thorleifsson G, Tyrer JP, Uh HW, Vandenput L, Verhulst FC, Vermeulen SH, Verweij N, Vonk JM, Waite LL, Warren HR, Waterworth D, Weedon MN, Wilkens LR, Willenborg C, Wilsgaard T, Wojczynski MK, Wong A, Wright AF, Zhang Q, Brennan EP, Choi M, Dastani Z, Drong AW, Eriksson P, Franco-Cereceda A, Gadin JR, Gharavi AG, Goddard ME, Handsaker RE, Huang J, Karpe F, Kathiresan S, Keildson S, Kiryluk K, Kubo M, Lee JY, Liang L, Lifton RP, Ma B, McCarroll SA, McKnight AJ, Min JL, Moffatt MF, Montgomery GW, Murabito JM, Nicholson G, Nyholt DR, Okada Y, Perry JR, Dorajoo R, Reinmaa E, Salem RM, Sandholm N, Scott RA, Stolk L, Takahashi A, Van't Hooft FM, Vinkhuyzen AA, Westra HJ, Zheng W, Zondervan KT, Heath AC, Arveiler D, Bakker SJ, Beilby J, Bergman RN, Blangero J, Bovet P, Campbell H, Caulfield MJ, Cesana G, Chakravarti A, Chasman DI, Chines PS, Collins FS, Crawford DC, Cupples LA, Cusi D, Danesh J, de Faire U, den Ruijter HM, Dominiczak AF, Erbel R, Erdmann J, Eriksson JG, Farrall M, Felix SB, Ferrannini E, Ferrieres J, Ford I, Forouhi NG, Forrester T, Franco OH, Gansevoort RT,Gejman PV, Gieger C, Gottesman O, Gudnason V, Gyllensten U, Hall AS, Harris TB, Hattersley AT, Hicks AA, Hindorff LA, Hingorani AD, Hofman A, Homuth G, Hovingh GK, Humphries SE, Hunt SC, Hypponen E, Illig T, Jacobs KB, Jarvelin MR, Jockel KH, Johansen B, Jousilahti P, Jukema JW, Jula AM, Kaprio J, Kastelein JJ, Keinanen-Kiukaanniemi SM, Kiemeney LA, Knekt P, Kooner JS, Kooperberg C, Kovacs P, Kraja AT, Kumari M, Kuusisto J, Lakka TA, Langenberg C, Le Marchand L, Lehtimaki T, Lyssenko V, Mannisto S, Marette A, Matise TC, McKenzie CA, McKnight B, Moll FL, Morris AD, Morris AP, Murray JC, Nelis M, Ohlsson C, Oldehinkel AJ, Ong KK, Madden PA, Pasterkamp G, Peden JF, Peters A, Postma DS, Pramstaller PP, Price JF, Qi L, Raitakari OT, Rankinen T, Rao DC, Rice TK, Ridker PM, Rioux JD, Ritchie MD, Rudan I, Salomaa V, Samani NJ, Saramies J, Sarzynski MA, Schunkert H, Schwarz PE, Sever P, Shuldiner AR, Sinisalo J, Stolk RP, Strauch K, Tonjes A, Tregouet DA, Tremblay A, Tremoli E, Virtamo J, Vohl MC, Volker U, Waeber G, Willemsen G, Witteman JC, Zillikens MC, Adair LS, Amouyel P, Asselbergs FW, Assimes TL, Bochud M, Boehm BO, Boerwinkle E, Bornstein SR, Bottinger EP, Bouchard C, Cauchi S, Chambers JC, Chanock SJ, Cooper RS, de Bakker PI, Dedoussis G, Ferrucci L, Franks PW, Froguel P, Groop LC, Haiman CA, Hamsten A, Hui J, Hunter DJ, Hveem K, Kaplan RC, Kivimaki M, Kuh D, Laakso M, Liu Y, Martin NG, Marz W, Melbye M, Metspalu A, Moebus S, Munroe PB, Njolstad I, Oostra BA, Palmer CN, Pedersen NL, Perola M, Perusse L,

Peters U, Power C, Quertermous T, Rauramaa R, Rivadeneira F, Saaristo TE, Saleheen D, Sattar N, Schadt EE, Schlessinger D, Slagboom PE, Snieder H, Spector TD, Thorsteinsdottir U, Stumvoll M, Tuomilehto J, Uitterlinden AG, Uusitupa M, van der Harst P, Walker M, Wallaschofski H, Wareham NJ, Watkins H, Weir DR, Wichmann HE, Wilson JF, Zanen P, Borecki IB, Deloukas P, Fox CS, Heid IM, O'Connell JR, Strachan DP, Stefansson K, van Duijn CM, Abecasis GR, Franke L, Frayling TM, McCarthy MI, Visscher PM, Scherag A, Wilier CJ, Boehnke M, Mohlke KL, Lindgren CM, Beckmann JS, Barroso I, North KE, Ingelsson E, Hirschhorn JN, Loos RJ, Speliotes EK, 2015 Genetic studies of body mass index yield new insights for obesity biology. Nature 518(7538), 197–206. [PubMed: 25673413]

Malpetti M, Sala A, Vanoli EG, Gianolli L, Luzi L, Perani D, 2018 Unfavourable gender effect of high body mass index on brain metabolism and connectivity. Sci. Rep. 8(1), 12584. [PubMed: 30135519]

Marioni RE, Yang J, Dykiert D, Mottus R, Campbell A, Davies G, Hayward C, Porteous DJ, Visscher PM, Deary IJ, 2016 Assessing the genetic overlap between BMI and cognitive function. Mol Psychiatry.

McEvoy LK, Fennema-Notestine C, Roddey JC, Hagler DJ Jr., Holland D, Karow DS, Pung CJ, Brewer JB, Dale AM, Alzheimer's Disease Neuroimaging I, 2009 Alzheimer disease: quantitative structural neuroimaging for detection and prediction of clinical and structural changes in mild cognitive impairment. Radiology 251(1), 195–205. [PubMed: 19201945]

Medic N, Ziauddeen H, Ersche KD, Farooqi IS, Bullmore ET, Nathan PJ, Ronan L, Fletcher PC, 2016 Increased body mass index is associated with specific regional alterations in brain structure. Int J Obes (Lond) 40(7), 1177–1182. [PubMed: 27089992]

Mora S, Musunuru K, Blumenthal RS, 2009 The clinical utility of high-sensitivity C-reactive protein in cardiovascular disease and the potential implication of JUPITER on current practice guidelines. Clin. Chem. 55(2), 219–228. [PubMed: 19095730]

Muthen LK, Muthen BO, 2015 Mplus User's Guide, 7 ed. Muthén & Muthén Los Angeles, CA.

Nam KN, Mounier A, Wolfe CM, Fitz NF, Carter AY, Castranio EL, Kamboh HI, Reeves VL, Wang J, Han X, Schug J, Lefterov I, Koldamova R, 2017 Effect of high fat diet on phenotype, brain transcriptome and lipidome in Alzheimer's model mice. Sci. Rep. 7(1), 4307. [PubMed: 28655926]

Olshansky SJ, Passaro DJ, Hershow RC, Layden J, Carnes BA, Brody J, Hayflick L, Butler RN, Allison DB, Ludwig DS, 2005 A potential decline in life expectancy in the United States in the 21st century. N Engl J Med 352(11), 1138–1145. [PubMed: 15784668]

Panizzon MS, Fennema-Notestine C, Eyler LT, Jernigan TL, Prom-Wormley E, Neale M, Jacobson K, Lyons MJ, Grant MD, Franz CE, Xian H, Tsuang M, Fischl B, Seidman L, Dale A, Kremen WS, 2009 Distinct genetic influences on cortical surface area and cortical thickness. Cereb. Cortex 19(11), 2728–2735. [PubMed: 19299253]

Panizzon MS, Hauger RL, Sailors M, Lyons MJ, Jacobson KC, Murray McKenzie R, Rana B, Vasilopoulos T, Vuoksimaa E, Xian H, Kremen WS, Franz CE, 2015 A new look at the genetic and environmental coherence of metabolic syndrome components. Obesity 23(12), 2499–2507. [PubMed: 26524476]

Pettigrew C, Soldan A, Zhu Y, Wang MC, Moghekar A, Brown T, Miller M, Albert M, Team BR, 2016 Cortical thickness in relation to clinical symptom onset in preclinical AD. Neuroimage Clin 12, 116–122. [PubMed: 27408796]

Reilly JJ, Kelly J, 2011 Long-term impact of overweight and obesity in childhood and adolescence on morbidity and premature mortality in adulthood: systematic review. Int J Obes (Lond) 35(7), 891–898. [PubMed: 20975725]

Reis JP, Allen N, Gunderson EP, Lee JM, Lewis CE, Loria CM, Powell - Wiley TM, Rana JS, Sidney S, Wei G, 2015 Excess body mass index - and waist circumference - years and incident cardiovascular disease: The CARDIA study. Obesity 23(4), 879–885. [PubMed: 25755157]

Richmond TK, Thurston I, Sonneville K, Milliren CE, Walls CE, Austin SB, 2015 Racial/ethnic differences in accuracy of body mass index reporting in a diverse cohort of young adults. Int J Obes (Lond) 39(3), 546–548. [PubMed: 25059116]

Santos CY, Snyder PJ, Wu WC, Zhang M, Echeverria A, Alber J, 2017 Pathophysiologic relationship between Alzheimer's disease, cerebrovascular disease, and cardiovascular risk: A review and synthesis. Alzheimers Dement (Amst) 7, 69–87. [PubMed: 28275702]

Santos PP, Silveira PS, Souza-Duran FL, Tamashiro-Duran JH, Scazufca M, Menezes PR, Leite CD, Lotufo PA, Vallada H, Wajngarten M, De Toledo Ferraz Alves TC., Rzezak P, Busatto GF, 2017 Prefrontal-Parietal White Matter Volumes in Healthy Elderlies Are Decreased in Proportion to the Degree of Cardiovascular Risk and Related to Inhibitory Control Deficits. Front. Psychol. 8, 57. [PubMed: 28184203]

Schoenborn CA, Heyman KM, 2009 Health characteristics of adults aged 55 years and over: United States, 2004-2007, in: U.S. Department of Health and Human Services Centers for Disease Control and Prevention (Ed.). Hyattsville, MD.

Shaw ME, Abhayaratna WP, Anstey KJ, Cherbuin N, 2017 Increasing Body Mass Index at Midlife is Associated with Increased Cortical Thinning in Alzheimer's Disease-Vulnerable Regions. J. Alzheimers Dis. 59(1), 113–120. [PubMed: 28550257]

Shaw ME, Sachdev PS, Abhayaratna W, Anstey KJ, Cherbuin N, 2018 Body mass index is associated with cortical thinning with different patterns in mid- and late-life. Int J Obes (Lond) 42(3), 455–461. [PubMed: 28993708]

Singh-Manoux A, Dugravot A, Shipley M, Brunner EJ, Elbaz A, Sabia S, Kivimaki M, 2018 Obesity trajectories and risk of dementia: 28 years of follow-up in the Whitehall II Study. Alzheimers Dement 14(2), 178–186. [PubMed: 28943197]

Sled JG, Zijdenbos AP, Evans AC, 1998 A nonparametric method for automatic correction of intensity nonuniformity in MRI data. IEEE Trans. Med. Imaging 17, 87–97. [PubMed: 9617910]

Tobi EW, Slieker RC, Luijk R, Dekkers KF, Stein AD, Xu KM, Biobank-based Integrative Omics Studies C, Slagboom PE, van Zwet EW, Lumey LH, Heijmans AT, 2018 DNA methylation as a mediator of the association between prenatal adversity and risk factors for metabolic disease in adulthood. Sci Adv 4(1), eaao4364. [PubMed: 29399631]

Twig G, Yaniv G, Levine H, Leiba A, Goldberger N, Derazne E, Ben-Ami Shor D, Tzur D, Afek A, Shamiss A, Haklai Z, Kark JD, 2016 Body-Mass Index in 2.3 Million Adolescents and Cardiovascular Death in Adulthood. N Engl J Med.

von Bonsdorff MB, Tormakangas T, Rantanen T, Salonen MK, Osmond C, Kajantie E, Eriksson JG, 2015 Early life body mass trajectories and mortality in older age: findings from the Helsinki Birth Cohort Study. Ann Med 47(1), 34–39. [PubMed: 25307361]

Vuoksimaa E, Panizzon MS, Chen CH, Fiecas M, Eyler LT, Fennema-Notestine A, Hagler DJ, Fischl B, Franz CE, Jak A, Lyons MJ, Neale MC, Rinker DA, Thompson WK, Tsuang MT, Dale AM, Kremen WS, 2015 The Genetic Association Between Neocortical Volume and General Cognitive Ability Is Driven by Global Surface Area Rather Than Thickness. Cereb Cortex 25(8), 2127–2137. [PubMed: 24554725]

Walhovd KB, Storsve AB, Westlye LT, Drevon CA, Fjell AM, 2014 Blood markers of fatty acids and vitamin D, cardiovascular measures, body mass index, and physical activity relate to longitudinal cortical thinning in normal aging. Neurobiol. Aging 35(5), 1055–1064. [PubMed: 24332985]

Willette AA, Kapogiannis D, 2015 Does the brain shrink as the waist expands? Ageing Res Rev 20, 86–97. [PubMed: 24768742]

Witte AV, Fobker M, Gellner R, Knecht S, Floel A, 2009 Caloric restriction improves memory in elderly humans. Proc. Natl. Acad. Sci. U. S. A. 106(4), 1255–1260. [PubMed: 19171901]

Xian H, Scherrer JF, Franz CE, McCaffery J, Stein PK, Lyons MJ, Jacobsen K, Eisen SA, Kremen WS, 2010 Genetic vulnerability and phenotypic expression of depression and risk for ischemic heart disease in the Vietnam era twin study of aging. Psychosom Med 72(4), 370–375. [PubMed: 20190130]

Xian H, Vasilopoulos T, Liu W, Hauger RL, Jacobson KC, Lyons MJ, Panizzon M, Reynolds CA, Vuoksimaa E, Kremen WS, Franz CE, 2017 Steeper change in body mass across four decades predicts poorer cardiometabolic outcomes at midlife. Obesity (Silver Spring) 25(4), 773–780. [PubMed: 28349665]

Xing CY, Tarumi T, Liu J, Zhang Y, Turner M, Riley J, Tinajero CD, Yuan LJ, Zhang R, 2017 Distribution of cardiac output to the brain across the adult lifespan. J. Cereb. Blood Flow Metab. 37(8), 2848–2856. [PubMed: 27789785]

HIGHLIGHTS

Body mass index/BMI trajectory across 4 decades predicts midlife cortical thickness Thinner temporal and frontal cortical ROIs in adults with steeply increasing BMI Midlife obesity associated with thinner cortex in similar regions Neither BMI trajectory nor obesity predicts white matter volume or abnormalities
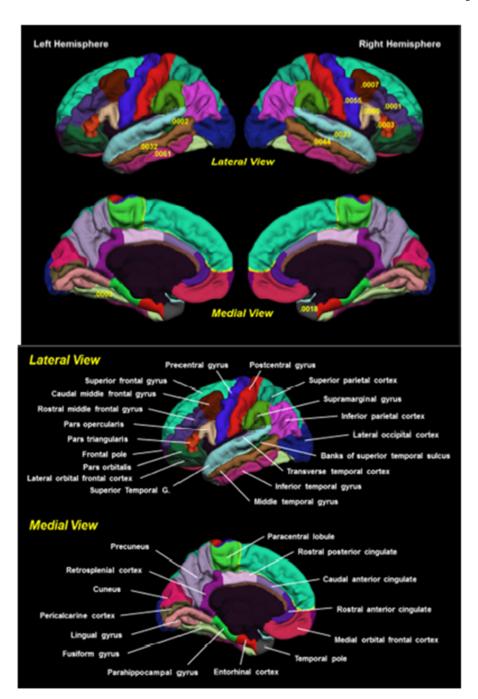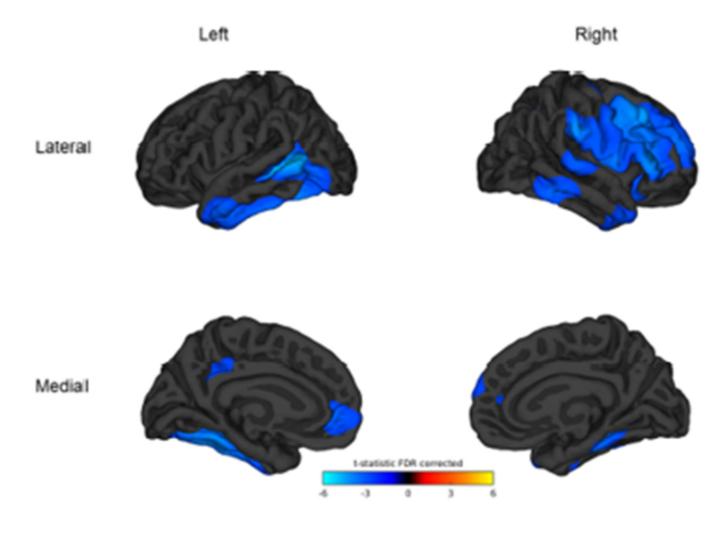
Figure 1.
Parcellation map of cortical regions associated with BMI trajectory by hemisphere (33 ROIs per hemisphere). Shown are p-values for regions that are significantly different in the obese versus the normal trajectory. All indicated ROIs are thinner for the obesity trajectory compared with the normal trajectory (see Table 2 for parameter estimates). T-1 weighted images were processed via the FreeSurfer v5.1 pipeline. Cortical parcellation data was derived from the Desikan-Killiany atlas (Desikan et al., 2006). Results adjusted for age, education, ethnicity, smoking, at-risk for hypertension, dyslipidemia, diabetes,

inflammation, and ischemic heart disease, and the random effect of family. Cortical thickness measures were adjusted for scanner and weighted average thickness.

Figure 2.
Vertex-wise comparisons by trajectory group. Blue color tones indicate areas in which the obesity trajectory is significantly thinner than the normal trajectory (t-test threshold > 2). Comparisons are significant at p<0.05, FDR corrected. Cortical vertex-wise analysis in conducted in Matlab r2014a using the Matlab FreeSurfer and Statistical toolboxes. Cortical thickness maps for each hemisphere were concatenated and a general linear mixed model was run contrasting the BMI trajectories (different intercept, different slope) while controlling education, ethnicity, age, risk for dyslipidemia, hypertension, diabetes, ischemic heart disease, and scanner. To improve sensitivity and signal to noise ratio, a 30 mm full wide half maximum smoothing kernel was applied as recommended (Lerch and Evans, 2005). Significance was set at p<.05 (FDR-corrected) for clusters larger than 100 voxels and statistic maps were rendered over the FreeSurfer average brain.

Table 1.

Demographics by BMI Trajectory

Variables (Mean/SD)	Normal Trajectory N=202 Mean (SD)	Obese Trajectory N=171 Mean (SD)	*p*-value
Age at MRI (Time 4)	62.0 (2.48)	61.7 (2.65)	*p*=0.20
Education (yrs)	14.0 (2.09)	13.7 (1.96)	*p*=0.24
AFQT Time 1	0.39 (0.67)	0.41 (0.68)	*p=0*.72
Ethnicity (% WNH)	90.8%	83.1%	*p*=0.03
BMI Time 1/Age 20, kg/m^2	21.4 (2.22)	23.7 (2.80)	*p*<0.0001
% obese	0%	3.5%	
BMI Time 2/Age 40, kg/m^2	23.6 (1.90)	27.4 (3.01)	*p*<0.0001
% obese	0%	10.5%	
BMI Time 3/age 56, kg/m^2	25.7 (2.41)	31.7 (2.92)	*p*<0.0001
% obese	2.9%	69.9%	
BMI Time 4/age 62, kg/m^2	25.9 (2.48)	32.6 (3.00)	*p*<0.0001
% obese	2.5%	82%	
Time 4/Age 62 Cardiometabolic risk factors			
C-Reactive Protein risk	18.7%	34.9%	*p*=0.01
Hypertension risk	59.7%	85%	*p*<0.0001
Diabetes risk	41.4%	58%	*p*=0.01
Hypercholestemia risk	58.5%	70.1%	*p*=0.03
Ischemic Heart Disease risk	10.2%	11.7%	*p*=0.66
Metabolic Syndrome risk	17.4%	59.4%	*p*<0.0001
Smoking			
% Never	86 (42.6)	66 (38.6)	*p* =0.29
% Former	74 (36.6)	76 (44.4)	
% Current	42 (20.8)	29 (17.0)	

Note. BMI= Body mass index; WNH=white non-Hispanic; AFQT=Armed Forces Qualification Test (Uhlaner JE, Bolanovich DJ. *Development of the Armed Forces Qualification Test and Predecessor Army Screening Tests, 1946-1950*. Washington, DC: Personnel Research Section, Department of the Army; 1952.)

Table 2.

Comparisons of cortical thickness regions of interest at Time 4 (~age 62) in normal versus obese BMI trajectory groups

Time 4/Age 62 MRI Regions of Interest	Left Hemisphere		Right Hemisphere		Bilateral	
	Point Estimate (95% CI)	p-value	Point Estimate (95% CI)	p-value	Point Estimate (95% CI)	p-value
Cingulate						
Isthmus of Cingulate Gyrus	−0.0280 (−0.0762, 0.0193)	0.2405	−0.0097 (−0.0570, 0.0377)	0.6864	−0.0141 (−0.0558, 0.0276)	0.5039
Caudal Anterior Cingulate	−0.0104 (−0.0741, 0.0533)	0.7475	−0.0340 (−0.0938, 0.0258)	0.2615	−0.0225 (−0.0725, 0.0276)	0.3748
Rostral Posterior Cingulate	−0.0304 (−0.0679, 0.0071)	0.1112	−0.0249 (−0.0646, 0.0149)	0.2171	−0.0268 (−0.0594, 0.0058)	0.1066
Rostral Anterior Cingulate	−0.0658 (−0.1210, −0.0105)	0.0201	−0.0399 (−0.0930, 0.0132)	0.1389	−0.0506 (−0.0952, −0.0059)	0.0267
Frontal Lobe						
Frontal Pole	−0.0612 (−0.1264, 0.0039)	0.0650	−0.0621 (−0.1275, 0.0033)	0.0627	**−0.0675 (−0.1211, −0.0140)**	**0.0149**[a]
Paracentral Lobule	0.0072 (−0.0299, 0.0443)	0.7000	−0.0105 (−0.0490, 0.0279)	0.5878	0.0020 (−0.0318, 0.0359)	0.9052
Precentral Gyrus	−0.0313 (−0.0701, 0.0076)	0.1133	**−0.0531 (−0.0903, −0.0160)**	**0.0055**[a]	−0.0424 (−0.0779, −0.0069)	0.0199
Superior Frontal Gyrus	−0.0142 (−0.0473, 0.0188)	0.3943	−0.0296 (−0.0604, 0.0012)	0.0598	−0.0201 (−0.0506, 0.0103)	0.1927
Pars Opercularis	−0.0132 (−0.0497, 0.0233)	0.4755	**−0.0556 (−0.0948, −0.0163)**	**0.0060**	−0.0343 (−0.0670, −0.0016)	0.0397
Pars Orbitalis	−0.0530 (−0.1054, −0.0006)	0.0473	0.0099 (−0.0379, 0.0577)	0.6819	−0.0234 (−0.0650, 0.0182)	0.2677
Pars Triangularis	−0.0317 (−0.0735, 0.0102)	0.1370	**−0.0673 (−0.1032, −0.0313)**	**0.0003**[a]	**−0.0481 (−0.0824, −0.0139)**	**0.0064**[a]
Caudal Middle Frontal Gyrus	−0.0274 (−0.0645, 0.0098)	0.1471	**−0.0692 (−0.1083, −0.0301)**	**0.0007**[a]	**−0.0475 (−0.0819, −0.0132)**	**0.0071**[a]
Rostral Middle Frontal Gyrus	−0.0362 (−0.0677, −0.0046)	0.0249	**−0.0575 (−0.0853, −0.0297)**	**0.0001**[a]	**−0.0464 (−0.0734, −0.0193)**	**0.0010**[a]
Lateral Orbitofrontal Cortex	−0.0277 (−0.0633, 0.0079)	0.1260	−0.0310 (−0.0688, 0.0067)	0.1058	−0.0304 (−0.0632, 0.0025)	0.0699
Medial Orbitofrontal Cortex	−0.0301 (−0.0694, 0.0092)	0.1314	−0.0150 (−0.0579, 0.0279)	0.4908	−0.0192 (−0.0537, 0.0153)	0.2729
Occipital Lobe						
Cuneus	0.0123 (−0.0175, 0.0422)	0.4139	−0.0064 (−0.0385, 0.0258)	0.6963	0.0029 (−0.0249, 0.0307)	0.8342
Lateral Occipital Cortex	−0.0105 (−0.0421, 0.0210)	0.5088	−0.0003 (−0.0336, 0.0330)	0.9851	−0.0044 (−0.0344, 0.0256)	0.7736
Lingual Gyrus	0.0091 (−0.0201, 0.0382)	0.5398	−0.0006 (−0.0302, 0.0290)	0.9703	0.0062 (−0.0206, 0.0331)	0.6473
Pericalcarine	0.0127 (−0.0157, 0.0411)	0.3785	−0.0027 (−0.0313, 0.0259)	0.8500	0.0038 (−0.0198, 0.0274)	0.7499
Parietal Lobe						
Inferior Parietal Cortex	−0.0179 (−0.0509, 0.0151)	0.2843	−0.0279 (−0.0612, 0.0054)	0.0997	−0.0216 (−0.0518, 0.0087)	0.1608
Postcentral Gyrus	−0.0217 (−0.0537, 0.0103)	0.1825	−0.0365 (−0.0659, −0.0071)	0.0154	−0.0276 (−0.0552, 0.0000)	0.0499
Precuneus	−0.0268 (−0.0580, 0.0043)	0.0907	−0.0234 (−0.0584, 0.0116)	0.1873	−0.0243 (−0.0547, 0.0060)	0.1150

Time 4/Age 62 MRI Regions of Interest	Left Hemisphere		Right Hemisphere		Bilateral	
	Point Estimate (95% CI)	p-value	Point Estimate (95% CI)	p-value	Point Estimate (95% CI)	p-value
Superior Parietal Cortex	0.0075 (−0.0269, 0.0420)	0.6657	−0.0023 (−0.0361, 0.0315)	0.8917	0.0070 (−0.0257, 0.0397)	0.6737
Supramarginal Gyrus	−0.0340 (−0.0696, 0.0016)	0.0607	−0.0388 (−0.0725, −0.0052)	0.0242	−0.0354 (−0.0661, −0.0048)	0.0240
Temporal Lobe						
Banks of Superior Temporal Sulcus	**−0.0739 (−0.1123, −0.0356)**	**0.0002[a]**	−0.0474 (−0.0890, −0.0059)	0.0255	**−0.0623 (−0.0931, −0.0315)**	**0.0001[a]**
Inferior Temporal Cortex	**−0.0492 (−0.0840, −0.0144)**	**0.0061[a]**	−0.0339 (−0.0695, 0.0017)	0.0620	**−0.0412 (−0.0719, −0.0105)**	**0.0090[a]**
Middle Temporal Gyrus	**−0.0521 (−0.0864, −0.0179)**	**0.0032[a]**	**−0.0500 (−0.0841, −0.0160)**	**0.0044[a]**	**−0.0503 (−0.0796, −0.0211)**	**0.0009[a]**
Superior Temporal Gyrus	−0.0336 (−0.0697, 0.0024)	0.0672	**−0.0556 (−0.0909, −0.0204)**	**0.0023[a]**	**−0.0410 (−0.0729, −0.0090)**	**0.0125[a]**
Transverse Temporal Gyrus	−0.0297 (−0.0842, 0.0249)	0.2832	−0.0407 (−0.0961, 0.0148)	0.1487	−0.0339 (−0.0817, 0.0138)	0.1616
Entorhinal Cortex	−0.0573 (−0.1387, 0.0241)	0.1656	−0.0240 (−0.1094, 0.0613)	0.5778	−0.0403 (−0.1103, 0.0298)	0.2569
Fusiform Gyrus	**−0.0650 (−0.0993, −0.0306)**	**0.0003[a]**	−0.0355 (−0.0692, −0.0018)	0.0389	**−0.0511 (−0.0815, −0.0207)**	**0.0012[a]**
Parahippocampal Gyrus	−0.0239 (−0.0989, 0.0511)	0.5280	−0.0502 (−0.1178, 0.0174)	0.1436	−0.0355 (−0.0996, 0.0286)	0.2747
Temporal Pole	−0.0652 (−0.1397, 0.0092)	0.0853	**−0.1130 (−0.1831, −0.0430)**	**0.0018[a]**	**−0.0867 (−0.1460, −0.0275)**	**0.0045[a]**

NOTE: Adjusted for scanner, age, ethnicity, education, smoking, at-risk for hypertension, diabetes, cholesterol, inflammation, ischemic heart disease and the random effect of family ID. MRI measures adjusted for scanner and weighted average thickness;

[a] indicates p<.05, FDR corrected. Negative sign indicates that the region is thinner in participants who are in the obese (BMI≥30) compared with those who are not obese (BMI <30) at Time 4 (age 62). Banks Sup Temporal Sulcus = Banks of Superior Temporal Sulcus.

Table 3.

Cross-sectional comparisons of cortical thickness regions of interest in obese versus non-obese groups at Time 4 (~age 62)

MRI measures (Regions of Interest)	Left Hemisphere Point Estimate (95% CI)	p-value	Right Hemisphere Point Estimate (95% CI)	p-value	Bilateral Point Estimate (95% CI)	p-value
Cingulate						
Isthmus of Cingulate Gyrus	−0.0259 (−0.0734, 0.0217)	0.2831	−0.0110 (−0.0587, 0.0366)	0.6477	−0.0155 (−0.0568, 0.0259)	0.4604
Caudal Anterior Cingulate	0.0191 (−0.0443, 0.0825)	0.5512	−0.0382 (−0.0984, 0.0220)	0.2108	−0.0105 (−0.0601, 0.0391)	0.6756
Rostral Posterior Cingulate	−0.0152 (−0.0526, 0.0222)	0.4210	−0.0070 (−0.0466, 0.0326)	0.7278	−0.0096 (−0.0417, 0.0225)	0.5543
Rostral Anterior Cingulate	−0.0805 (−0.1364, −0.0246)	0.0052	−0.0229 (−0.0770, 0.0311)	0.4020	−0.0491 (−0.0941, −0.0041)	0.0330
Frontal Lobe						
Frontal Pole	−0.0703 (−0.1362, −0.0045)	0.0366	−0.0520 (−0.1176, 0.0136)	0.1190	−0.0646 (−0.1181, −0.0112)	0.0183
Paracentral Lobule	−0.0162 (−0.0528, 0.0205)	0.3833	−0.0342 (−0.0720, 0.0036)	0.0756	−0.0227 (−0.0559, 0.0104)	0.1761
Precentral Gyrus	−0.0397 (−0.0791, −0.0004)	0.0480	**−0.0607 (−0.0980, −0.0234)**	**0.0017[a]**	**−0.0502 (−0.0859, −0.0145)**	**0.0063[a]**
Superior Frontal Gyrus	−0.0111 (−0.0435, 0.0213)	0.4970	−0.0230 (−0.0533, 0.0073)	0.1357	−0.0151 (−0.0448, 0.0147)	0.3182
Pars Opercularis	−0.0187 (−0.0557, 0.0182)	0.3171	−0.0461 (−0.0861, −0.0060)	0.0246	−0.0311 (−0.0642, 0.0020)	0.0654
Pars Orbitalis	−0.0456 (−0.0984, 0.0072)	0.0899	0.0250 (−0.0229, 0.0730)	0.3029	−0.0083 (−0.0498, 0.0332)	0.6927
Pars Triangularis	−0.0379 (−0.0797, 0.0040)	0.0760	**−0.0770 (−0.1135, −0.0405)**	**0.0001[a]**	**−0.0562 (−0.0905, −0.0220)**	**0.0015[a]**
Caudal Middle Frontal Gyrus	−0.0453 (−0.0825, −0.0081)	0.0176	**−0.0586 (−0.0982, −0.0190)**	**0.0042[a]**	**−0.0509 (−0.0852, −0.0165)**	**0.0041[a]**
Rostral Middle Frontal Gyrus	−0.0229 (−0.0544, 0.0087)	0.1536	**−0.0586 (−0.0865, −0.0308)**	**0.0001[a]**	**−0.0395 (−0.0665, −0.0126)**	**0.0045[a]**
Lateral Orbitofrontal Cortex	−0.0294 (−0.0648, 0.0061)	0.1038	−0.0177 (−0.0559, 0.0205)	0.3608	−0.0224 (−0.0554, 0.0105)	0.1793
Medial Orbitofrontal Cortex	−0.0337 (−0.0731, 0.0058)	0.0933	−0.0071 (−0.0499, 0.0357)	0.7422	−0.0182 (−0.0523, 0.0160)	0.2949
Occipital Lobe						
Cuneus	0.0039 (−0.0262, 0.0341)	0.7968	−0.0078 (−0.0401, 0.0244)	0.6308	−0.0012 (−0.0290, 0.0267)	0.9334
Lateral Occipital Cortex	−0.0106 (−0.0420, 0.0209)	0.5069	0.0145 (−0.0184, 0.0474)	0.3830	0.0032 (−0.0264, 0.0328)	0.8293
Lingual Gyrus	0.0173 (−0.0115, 0.0462)	0.2360	0.0140 (−0.0154, 0.0435)	0.3470	0.0189 (−0.0075, 0.0453)	0.1580
Pericalcarine	0.0029 (−0.0257, 0.0314)	0.8418	0.0131 (−0.0155, 0.0418)	0.3657	0.0082 (−0.0152, 0.0316)	0.4882
Parietal Lobe						
Inferior Parietal Cortex	−0.0214 (−0.0541, 0.0112)	0.1957	−0.0298 (−0.0633, 0.0036)	0.0799	−0.0248 (−0.0548, 0.0052)	0.1040
Postcentral Gyrus	−0.0214 (−0.0534, 0.0106)	0.1883	**−0.0499 (−0.0788, −0.0210)**	**0.0009[a]**	−0.0325 (−0.0597, −0.0052)	0.0200
Precuneus	−0.0436 (−0.0744, −0.0127)	0.0061	−0.0242 (−0.0591, 0.0107)	0.1727	−0.0317 (−0.0618, −0.0016)	0.0395

MRI measures (Regions of Interest)	Left Hemisphere		Right Hemisphere		Bilateral	
	Point Estimate (95% CI)	p-value	Point Estimate (95% CI)	p-value	Point Estimate (95% CI)	p-value
Superior Parietal Cortex	0.0075 (−0.0269, 0.0420)	0.6657	−0.0023 (−0.0361, 0.0315)	0.8917	0.0060 (−0.0258, 0.0379)	0.7076
Supramarginal Gyrus	−0.0326 (−0.0684, 0.0032)	0.0741	**−0.0586 (−0.0922, −0.0250)**	**0.0008**[a]	**−0.0443 (−0.0749, −0.0137)**	**0.0050**[a]
Temporal Lobe						
Banks Sup Temporal Sulcus	**−0.0547 (−0.0943, −0.0151)**	**0.0072**[a]	−0.0259 (−0.0681, 0.0162)	0.2251	**−0.0394 (−0.0707, −0.0081)**	**0.0142**[a]
Inferior Temporal Cortex	**−0.0478 (−0.0829, −0.0127)**	**0.0081**[a]	−0.0301 (−0.0653, 0.0051)	0.0930	−0.0371 (−0.0676, −0.0067)	0.0174
Middle Temporal Gyrus	**−0.0486 (−0.0831, −0.0142)**	**0.0061**[a]	**−0.0475 (−0.0818, −0.0132)**	**0.0071**[a]	**−0.0473 (−0.0766, −0.0180)**	**0.0018**[a]
Superior Temporal Gyrus	−0.0381 (−0.0740, −0.0021)	0.0382	**−0.0622 (−0.0972, −0.0271)**	**0.0007**[a]	**−0.0480 (−0.0796, −0.0164)**	**0.0033**[a]
Transverse Temporal Gyrus	−0.0409 (−0.0955, 0.0138)	0.1409	−0.0440 (−0.1000, 0.0120)	0.1222	−0.0415 (−0.0892, 0.0062)	0.0877
Entorhinal Cortex	−0.0666 (−0.1488, 0.0157)	0.1114	−0.0539 (−0.1398, 0.0321)	0.2171	−0.0601 (−0.1302, 0.0101)	0.0926
Fusiform Gyrus	**−0.0549 (−0.0894, −0.0205)**	**0.0021**[a]	−0.0353 (−0.0690, −0.0016)	0.0405	**−0.0453 (−0.0756, −0.0150)**	**0.0038**[a]
Parahippocampal Gyrus	−0.0347 (−0.1091, 0.0397)	0.3573	−0.0424 (−0.1106, 0.0258)	0.2204	−0.0360 (−0.1000, 0.0279)	0.2664
Temporal Pole	−0.0516 (−0.1264, 0.0231)	0.1736	**−0.0957 (−0.1668, −0.0246)**	**0.0088**[a]	−0.0663 (−0.1256, −0.0070)	0.0289

NOTE: Adjusted for scanner, age, ethnicity, education, smoking, at-risk for hypertension, diabetes, cholesterol, inflammation, ischemic heart disease and the random effect of family ID. MRI measures adjusted for scanner and weighted average thickness;

[a] indicates p<.05, FDR corrected. Negative sign indicates that the region is thinner in participants who are in the obese (BMI≥30) compared with those who are not obese (BMI < 30) at Time 4 (age 62). Banks Sup Temporal Sulcus = Banks of Superior Temporal Sulcus.